American Mineralogist, Volume 83, pages 1152–1160, 1998

Ruthenium solubility in hematite

CHRISTOPHER J. CAPOBIANCO*

Lunar and Planetary Laboratory, University of Arizona, Tucson, Arizona 85721–0092, U.S.A.

ABSTRACT

Solid binary oxides of the platinum-group elements (PGE) decompose on heating in air to metal, oxygen, and often, a mixture of volatile PGE oxides. Compared to most other transition metal oxides, these decomposition temperatures are low, generally below 1100 °C. The modest exception is RuO_2, which remains stable in air until 1400 °C. Because of its comparatively high oxide stability, Ru, among all the PGE, is the one with the greatest potential for a significant oxidic, i.e., lithophile, geochemistry. A series of 1 atm phase equilibrium experiments were made to establish the limits of solid solution of Ru in hematite (Fe_2O_3) and help evaluate the significance of the oxidic geochemistry of Ru.

The solid-solution limit for Ru in hematite may be represented by the following oxidation-reduction reaction:

$$2RuO_2 + Fe_2O_3 = 2FeRuO_3 + 1/2O_2.$$

Experiments equilibrated between 1012 and 1490 °C were buffered with respect to oxygen fugacity by the coexistence of Ru metal and solid RuO_2, both as essentially pure phases. Solution of Ru in hematite is enhanced at lower oxygen fugacity, but reaches a maximum fixed by the presence of Ru metal. An endothermic enthalpy for the reaction (188.1 ± 0.7 kJ/mol) was retrieved from the redox-controlled solubilities was as a regular solution interaction parameter (18.5 ± 0.5 kJ/mol) that indicated small positive deviations from ideality in the solid-solution region investigated. Estimates based on the new data for solubilities of Ru in a rhombohedral oxide at geologic conditions suggest that natural concentrations might be accommodated at high temperatures without saturation in Ru metal, but that exsolution of Ru metal from oxides would be favored at low temperature.

INTRODUCTION

A basis for understanding the oxidic geochemistry of Ru begins with what is known about the solid-state chemistry of its oxide compounds. Most of that research, motivated by technological issues, lies outside the geosciences literature, however. As a starting point for interpreting the oxidic geochemistry of Ru, research efforts from other venues are briefly described. Research concerning electronic applications of RuO_2, e.g., thick-film resistors (Hrovat et al. 1993; Hrovat et al. 1996) and anode coatings for electrolytic production of chlorine (Beer 1980), stems from the unusual metallic conductivity of RuO_2. One of the radioactive isotopes of Ru, ^{106}Ru, has attracted the attention of the nuclear waste management community because it is a decay product in high-level nuclear waste, and can be present up to several wt% in the borosilicate glass wasteform (Dixon et al. 1980; van Berkel et al. 1987; Schreiber et al. 1986; Jantzen et al. 1981; Hutson 1994). The occurrence of perovskite-derivative crystal structures of Ru oxide compounds analogous to those of known high T_c superconductors has sparked much of the research on oxidic Ru compounds from the materials science community (Williams et al. 1991; Quilty et al. 1993; Randall and Ward 1959; Donohue et al. 1966; Kafalas and Longo 1970; Longo and Kafalas 1968; Kobayashi et al. 1994). Ru-bearing perovskites have also been examined for applications in several types of industrial catalysts (Wiley and Poeppelmeier 1991; Greatrex et al. 1979). The single most important geochemical fact distilled from this body of work is the dominance of Ru^{4+} in oxidic compounds.

The thermodynamic instability of the lower oxidation states of Ru was discussed by Wiley and Poeppelmeier (1991) to explain their inability to synthesize oxygen deficient Ru-bearing perovskites for catalysis. Although spectroscopic data indicates that other oxidation states (Ru^{2+}, Ru^{3+}, Ru^{5+}) can exist in oxides (e.g., Triggs et al. 1984; Blazey et al. 1985), species other than 4+ generally occur in mixed-valence phases dominated by Ru^{4+}. Exceptions exist, however, and Ru^{5+} and even Ru^{7+} occur in oxide compounds where they are essential structural constituents and the only Ru species (e.g., Silverman and Levy 1954; and Greatrex et al. 1979; Battle et al. 1989). For this reason, a more precise generalization and one most relevant to the geochemistry of Ru, is that Ru^{4+} is

* Current address: 125 Fox Chase Rd., Asheville, NC 28804, U.S.A. E-mail: chrisc@lpl.arizona.edu

0003–004X/98/1112–1152$05.00

the *lowest* valence in oxides that is not induced by special defect equilibria. Although cationic valence is always important to the geochemistry of an element, it carries especial significance for Ru and the other PGE which, due to their chemical nobility, might possess no oxidic geochemistries at all depending on the identity of their lowest stable oxidation state.

At a typical magmatic temperature and oxygen fugacity, e.g., that imposed by the assemblage quartz-magnetite-fayalite (QMF), pure Ru metal is stable relative to its oxide. But even at QMF, the activity of the Ru oxide component is not zero. The activity of the oxidized Ru component may be small, but so too is the natural concentration of Ru. It may be that the natural concentration is small enough to allow a large fraction of it to be present in the oxidized form. Of course, this presupposes the absence of non-oxidic phases that could consume available Ru, e.g., sulfide. Furthermore, thermodynamics of mixing an oxidic Ru component in a geologic host phase must not produce strongly positive deviations from ideality. For example, if the relevant oxidation state yields a geochemically incompatible cation, metallic saturation may occur at concentrations that are low even compared with natural concentrations.

Another reason that the lowest likely oxidation state of Ru is geochemically important can be understood by the following redox reaction:

$$\mathrm{Ru} + \frac{n}{4}\mathrm{O}_2 \leftrightarrow \mathrm{Ru}^{n+}\mathrm{O}_{n/2} \qquad (1)$$

The equilibrium constant, K_1, is given in logarithmic form

$$\ln K_1 = \ln\frac{a_{\mathrm{Ru}^{n+}\mathrm{O}_{n/2}}}{a_{\mathrm{Ru}}} - n/4 \ln f_{\mathrm{O}_2} \qquad (2)$$

where a_i is the activity of component i referenced to pure solid phases at T and P, and n is the oxidation number of i in the oxidic component. Under the condition of saturation in metallic Ru, the activity of the oxidized Ru component is related to the oxygen fugacity raised to the $n/4$ power. If n is large, the saturation activity for the $\mathrm{Ru}^{n+}\mathrm{O}_{n/2}$ component decreases strongly with decreasing oxygen fugacity (e.g., O'Neill et al. 1995). If n is too large, the activity may be so small at geologically relevant values of f_{O_2} as to be quantitatively negligible.

Whether an oxidic geochemistry for Ru^{4+} exists at geologic conditions depends on several factors: (1) the intrinsic thermodynamic stability of RuO_2 components; (2) the solid-solution interactions of these components with host phases; and (3) the comparative stability of lower oxidation states for Ru . A simple evaluation of the intrinsic stabilities of oxidized PGE components is shown in Figure 1. Estimates for the equilibrium constants of reactions such as Equation 1 were made using tabulated enthalpies and entropies for solid oxide and metallic PGE phases (Westland 1989) to calculate a standard-state Gibbs free energy change over a range of temperatures. Activities for PGE oxide components are plotted for the oxygen fugacity given by QMF and at saturation in the metallic PGE phase. For oxide activities that lie above the calculated saturation curve, PGE oxide components must coexist with a metallic PGE phase; below each curve, the PGE could be contained entirely in oxidized form. As expected for easily reducible oxides, calculated saturation activities are very low (note the ordinate is on a parts per billion scale). The shaded region on this diagram is the regime of natural concentrations for the PGE (typically <10 ppb), which of course excludes ore bodies. Assuming the presence of a phase in which the PGE oxide component mixes ideally, Figure 1 indicates that natural concentrations of most PGE, and in particular Ru, could be entirely accommodated without reaching saturation in the metallic phase. [Peach and Mathez (1996) made an analogous observation based on their experiments concerning the solubility Ir in sulfide, which is so large that natural Ir concentrations would be insufficient to precipitate Ir metal.] Thus, Figure 1 illustrates that for an oxygen fugacity defined by QMF, there is no need to call upon any less stable, or unusual, lower oxidation states for most of the PGE in magmas—it seems that the saturation activities for the normal oxide PGE components are, for the most part, well above the natural concentration levels.

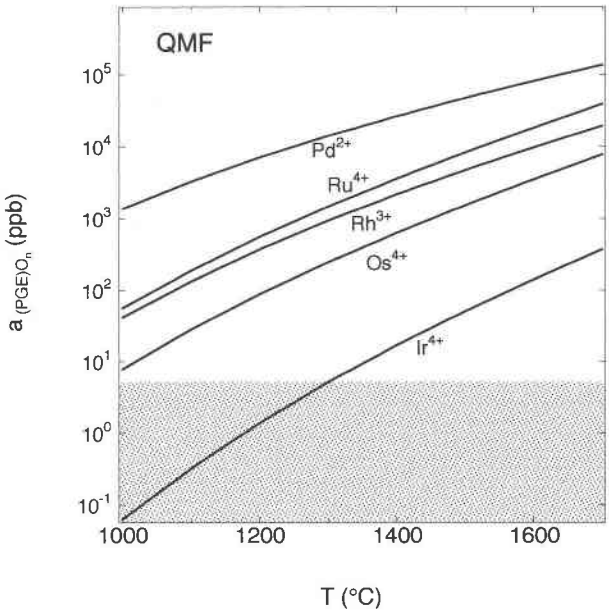

FIGURE 1. PGE oxide component activities are plotted for saturation in PGE metal and at the oxygen fugacity imposed by quartz-magnetite-fayalite (QMF) oxygen buffer. Thermodynamic data to calculate equilibrium constants for the solid oxides were taken from Westland (1989). Shaded region represents regime of PGE concentrations in (non-ore) terrestrial rocks. Although the activities are low (note the parts per billion scale), normal oxide component activities are generally above the natural concentration levels.

Recently, Capobianco et al. (1994) and Capobianco and Drake (1990) investigated the crystal/silicate-melt partitioning behavior of Ru for several igneous oxide phases: magnetite, hematite, ilmenite, and spinel. They

reported large crystal-chemical compatibilities for Ru, i.e., crystal/melt partition coefficients $\gg 1$. But those experiments were carried out at high oxygen fugacities to allow concentrations to be measured easily and were therefore unlike typical magmatic conditions. Extrapolation of their results to geologically relevant oxygen fugacity requires information on the thermodynamics of the Ru component in the phases of interest. To help evaluate the role of oxide phases in the magmatic geochemistry of Ru, I report here new phase equilibrium data on the RuO_2-Fe_2O_3 system. Solubility relationships of Ru in hematite were examined in a series of polythermal experiments at the redox condition imposed by the Ru + ½ O_2 = RuO_2 reaction. This oxygen fugacity constraint enables a simple characterization of the thermodynamic properties for the solid-solution limit of Ru in hematite.

Experimental methods

At elevated temperatures in an oxidizing atmosphere, such as air, RuO_2 is volatile as the gaseous species, RuO_3 and RuO_4 (Rard 1985). For this reason investigations involving high-temperature reactions of RuO_2 with other solids are best conducted using closed containers. Two methods of encapsulation were tried, welded $Au_{75}Pd_{25}$ capsules and evacuated silica glass tubes.

Starting materials

Powders of reagent grade Fe_2O_3, Ru metal (200 mesh) and RuO_2 (prepared by heating the metal powder at 900 °C in air overnight) were mixed under acetone in an agate mortar and pestle. Mixed powders were pressed into compacted pellets using a die set and a small hydraulic hand press. Fragments of these pellets were used for starting materials.

Experimental procedures

Noble metal alloy ($Au_{75}Pd_{25}$) capsules were fabricated from tubes ~15 mm in length, 3 mm OD. Capsules were welded at one end, loaded with starting material, flattened to allow for thermal expansion of enclosed gases, and welded shut. These were suspended in a resistance-heated, vertical tube furnace with $MoSi_2$ elements. Temperature was monitored by adjacent R-type Pt/Rh thermocouples that are routinely calibrated against the melting point of Au. Run conditions were maintained within ±2 °C. Samples were quenched by rapid withdrawal of the run assembly from the furnace and subsequently cooled in air.

Evacuated silica glass tube experimental assemblies (Fig. 2) provided a method far superior to welded capsules for determination of equilibrium solubilities in a closed and well-defined system. Starting materials were held in alumina crucibles inside evacuated silica glass tubes to prevent reaction of hematite with silica glass. Thick-walled (1.5–2.0 mm) silica glass tubes were used to allow runs at temperatures as high as 1490 °C. This high temperature is well above the traditional limit for silica glass tubes but was sustainable for about 4 h without devitrification. In all the silica glass tube experiments, fresh laboratory air was pumped continuously through the alumina muffle tube during the experiment. This technique seemed essential to prevent devitrification of the silica glass at high temperature, presumably by flushing out contaminants that might become nucleation sites for devitrification.

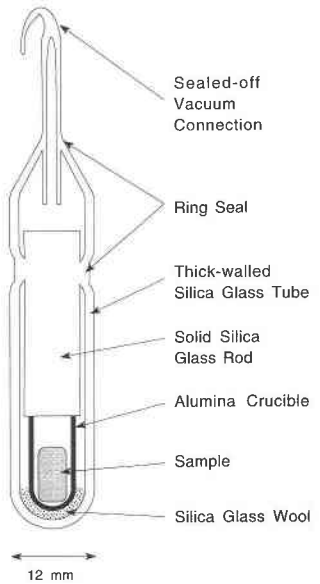

Figure 2. Evacuated silica glass tube assembly used in experiments. A solid silica glass rod, which is ring-seal welded in place, reduces the volume available to the sample to give a more isothermal system. Because the silica rod is fixed, the silica glass wool shown at the bottom of the tube is necessary to alleviate thermal stress that would otherwise cause the tube to break during heating. Note, the smaller OD silica tube is attached to permit easier sealing off of the system from the vacuum system.

Experiment duration varied with temperature and ranged from 336 h at 1012 °C to 1.5 h at 1490 °C. In most experiments, the Ru-bearing hematite was formed by synthesis from pure phases in the starting material. In two cases, the equilibrium solid solution was approached in the reverse manner, i.e., by decomposition of a previously synthesized Ru-bearing hematite. Re-equilibration temperatures of material used in reversal experiments were lower than the initial synthesis temperatures. The starting material in the reversal experiments was therefore oversaturated in Ru and exsolution was induced. In one of these runs, the noble metal capsule technique was used while in the other, the silica glass tube technique was used. The silica glass tube reversal run temperature was selected to be the same as one of the earlier synthesis runs; a direct comparison of solubilities was therefore possible in that case.

Product characterization

Quenched samples were first examined under a binocular optical microscope, then mounted in epoxy, and polished for reflected light optical microscopy and electron microprobe analysis. Portions of most samples were reserved for X-ray powder diffraction to confirm hematite crystal struc-

TABLE 1. Ru solubility in hematite at 1 bar and with f_{O_2} buffered by Ru-RuO_2

Exp. no.	Capsule	Duration (h)	T (°C)	Ru wt%	Total
367	AuPd	336	1012	10.61 ± 0.81*	98.25 ± 0.79†
405	silica	312	1050	12.43 ± 0.41	97.07 ± 0.56
409	silica	216	1125	15.55 ± 0.71	99.04 ± 0.40
395-R‡	AuPd	192	1152	18.97 ± 0.34	98.8 ± 0.66
410	silica	216	1175	19.36 ± 0.77	98.74 ± 0.61
411	silica	156	1228	22.28 ± 0.42	101.15 ± 0.67
427-R§	silica	164	1228	22.63 ± 0.62	97.86 ± 0.73
417	silica	39	1300	26.73 ± 0.42	100.10 ± 1.06
416	silica	21	1349	28.11 ± 0.22	99.64 ± 0.49
419	silica	21	1350	28.49 ± 0.60	99.53 ± 0.90
421	silica	18	1360	28.71 ± 0.18	100.17 ± 0.58
382	silica	12	1405	31.30 ± 0.22	99.35 ± 0.60
383	silica	3	1445	33.07 ± 0.19	100.14 ± 0.55
393	silica	1.5	1490	33.82 ± 0.21	98.98 ± 0.46

* One standard deviation of at least 10 electron microprobe analyses.
† Total based on trivalent Ru and Fe.
‡ Portion of no. 393 used as starting material.
§ Portion of no. 382 and additional Ru/Ru-oxide buffer used as starting material.

ture and to check for ilmenite-type ordering reflections. An electron microprobe was used at 15 kV and 10 nA to determine chemical composition. Pure Ru and Fe metals were used as standards. Backscattered electron (BSE) imaging and quantitative analysis were used to assess phase homogeneity, to measure solid solution of Ru in hematite, and to evaluate the purity of other coexisting phases.

Electron microprobe analytical totals were based on the oxide components Fe_2O_3 and Ru_2O_3. This is not meant to imply that both Fe and Ru are wholly trivalent; as discussed below, this is unlikely. Oxide totals using Fe_2O_3 and RuO_2 would produce totals >100% under optimal analytical conditions because of the non-stoichiometric excess of oxygen. In fact, the analytical total depends on the quality of the polished surface and the carbon coating. In these experiments the surface of the sample was typically porous and high-quality polished surfaces were not obtained. Thus, most analytical totals are <100% even though there are no appreciable impurities (the impurity of greatest concentration is <0.05 wt% Al). Though considered unlikely, low or high totals could also result if valences states for Ru greater than 4+ or less than 3+, respectively, existed in the solid solution.

RESULTS AND DISCUSSION

Evidence for equilibrium

Many experiments conducted in this study did not result in an equilibrium assemblage (these experiments are not reported in Table 1). Nevertheless, useful qualitative information was obtained in several instances to indicate a plausible reaction mechanism. Petrographic examination of failed experiments revealed several modes of disequilibrium. Most failed experiments were carried out in noble metal capsules and these yielded petrographic textures that varied across the sample. Typically, exsolution textures in these experiments were found in the cores of hematite grains but not in the rims. Changes in redox conditions throughout the run, possibly due to alloying of metallic Ru with the capsule wall, could account for this effect. An example of a failed run is shown in a BSE image in Figure 3. Other products of failed experiments revealed compositional variability within the hematite

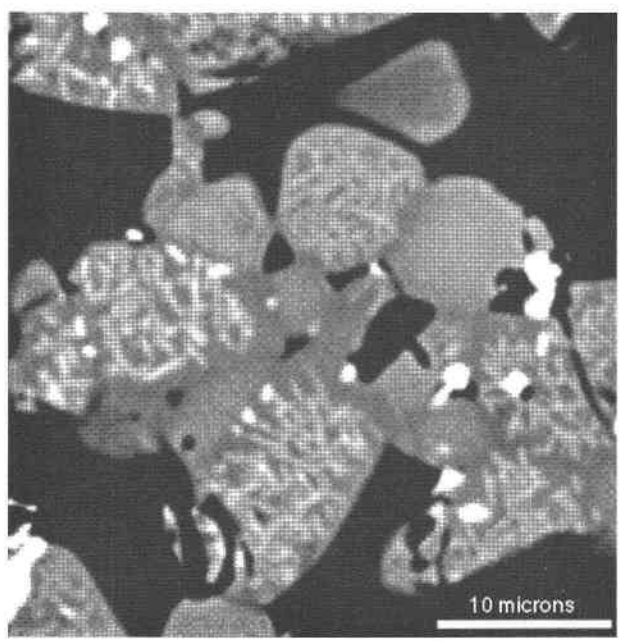

FIGURE 3. BSE image of a sintered sample of Ru-bearing hematite showing unequilibrated texture. Exsolved crystals of RuO_2 are found in a Widmanstatten-like pattern within some, but not all grains. Variations in contrast within grains are due to variable Ru content. Texture is suspected to arise by oxygen fugacity variation throughout a run of insufficient duration.

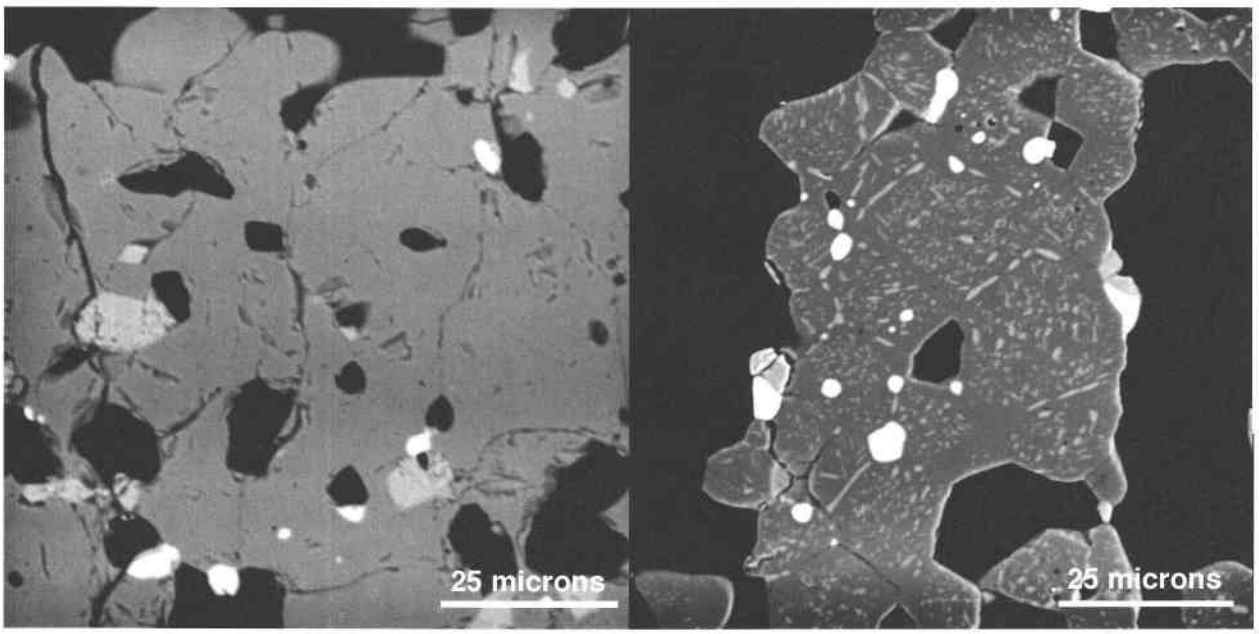

FIGURE 4. (A) Equilibrated texture produced in a synthesis run (382). All phases show homogeneous and uniform BSE contrast: brightest phase is Ru metal, intermediate gray is RuO_2 and the darkest gray, major phase, is Ru-bearing hematite. (B) Texture of equilibrium reversal run (427). Note that exsolved RuO_2 crystals are distributed relatively homogeneously and, because of their rounded appearance, seem to be better annealed. Also there is no BSE contrast attributable to compositional heterogeneity.

grains. These experiments were not held at run conditions long enough. In still other failed runs, the absence of one of the buffering phases produced hematite that was either too oxidized or too reduced.

The absence of petrographic evidence for disequilibrium as well as the presence of both redox-buffering phases were qualitative indicators of a successful experiment. Typical products of successful experiments are shown in the BSE image of Figure 4. The absence of contrast variation in BSE images of individual crystals and measured compositional homogeneity were additional requirements for a successful run.

Compositional information on the hematite solid solutions can also be used to assess the approach to equilibrium. Table 1 and Figure 5 report and plot the solubilities of Ru in hematite obtained from successful experiments. The strongest evidence for equilibrium comes from the precise overlap of the synthesis run no. 411 and the reversal run no. 427-R. The other reversal run no. 395-R also plots close to a value expected from nearby synthesis runs. Furthermore run numbers 416, 419, and 421, which are nearly isothermal and therefore represent replicate runs, show good internal agreement.

In general, equilibrium was more easily approached in this system than in the analogous system Fe_2O_3-TiO_2 (Lindsley 1991). Enhanced kinetics in the Ru-bearing system may be due to its much higher vapor pressures. Commonly, RuO_2 crystals in the run product are large and sharply faceted, indicative of growth from a vapor. In the Ru-bearing system, chemical vapor transport seems to have a fluxing action on the hematite solid solution that produces homogeneous solid solutions, provided the conditions are kept constant, even at relatively low temperature (1000 °C).

A further indication that vapor fluxing helped to achieve equilibrium was its absence in an exploratory 10 kbar piston-cylinder run using a $Au_{75}Pd_{25}$ capsule. In this experiment (3 days at 1000 °C) the interiors of hematite grains were nearly devoid of Ru (<0.1 wt% Ru) whereas the grain edges contained up to 8 wt% Ru. Such gradients are expected from solid state bulk and grain boundary diffusion-limited processes and are unlike the disequilibrium textures described from 1 atm experiments that showed exsolution of previously enriched grain cores or turbidity contrast in BSE images. This difference in disequilibrium textures is plausibly attributed to the absence of vapor in the high-pressure experiment and reinforces the hypothesis of vapor-assisted equilibration.

Reaction mechanism

The oxygen fugacity of unbuffered experiments, in which only hematite and RuO_2 were found in the products, was higher than that imposed by the following equilibrium:

$$RuO_2 = Ru + O_2. \quad (3)$$

Microprobe analyses found these hematites to be Ru-poor compared to isothermal experiments in which both solids of Equation 3 were present in the product. A chemical reaction that accommodates the qualitative observation that over-oxidation produces lower Ru saturation concentrations in hematite is the following:

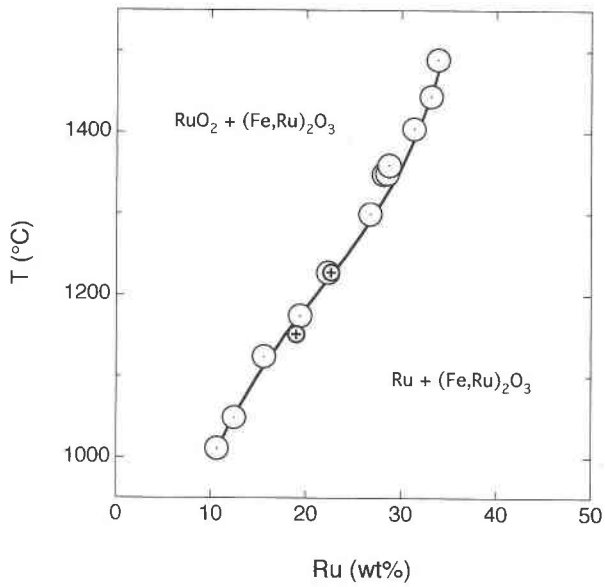

FIGURE 5. Temperature dependence of experimental solubilities of Ru in hematite buffered at an oxygen fugacity given by Ru + O_2 = RuO_2. Curve is fitted based on a two-parameter thermodynamic model described in text. All experiments are synthesis runs except the two shown by special symbols, which are reversals. Compositional error estimates (one sigma) based on microprobe analyses are smaller than symbols.

$$2RuO_2 + Fe_2O_3 = 2FeRuO_3 + 1/2O_2. \quad (4)$$

Here reaction products are oxygen and an ilmenite-like component, $FeRuO_3$. Like ilmenite, this Ru-bearing ilmenite component is favored at lower oxygen fugacity, as long as RuO_2 is stably present. Whether the Ru-bearing ilmenite component is like ilmenite in cation valences, i.e., with divalent and quadrivalent cations, is not yet known with certainty. The oxidation state of both Fe and Ru in the product is ambiguous in Equation 4.

Although it is likely that all four possible species (Ru^{4+}, Ru^{3+}, Fe^{3+}, and Fe^{2+}) are present in the hematites, several lines of independent evidence suggest that Ru^{4+} dominates the Ru species, necessitating the reduction of Fe^{3+} to Fe^{2+}. First, as mentioned above, evidence from the literature on Ru oxide chemistry indicates that quadrivalency predominates. Second, the solubility of Ru in hematite increases with increasing temperature in concert with the potential for Fe^{2+}. This potential is evident from the disproportionation of hematite to magnetite and oxygen as temperature is raised. Thus, by incorporating Ru^{4+}, hematite can satisfy the chemical tendency for Fe^{3+} reduction without transformation to magnetite. In fact, magnetite, if pure, would be the stable phase at the highest temperature investigated in this study (1490 °C), but instead an Ru-bearing hematite phase was recovered. Apparently, the thermal stability of the hematite structure is enhanced by incorporation of Ru^{4+} cations. This would not be expected if Ru^{3+} were the soluble species, since Ru_2O_3 is not a stable phase (Rard 1985).

A third indication of the probable predominance of Ru^{4+} over Ru^{3+} in hematite comes by analogy with several unpublished experiments identical to the 1350 °C noble metal capsule experiments reported here, except that Cr_2O_3 was used instead of Fe_2O_3. Whereas the Fe-bearing system dissolved ~28 wt% Ru, the Cr-bearing system, in which only trivalent chromium is likely, can accommodate only ~3–4 wt% Ru. If most of the Ru dissolved in Cr_2O_3 is Ru^{3+}, then this more limited solubility provides an estimate of how much Ru^{3+} might be present in the isostructural hematite. But comparisons between isostructural phases having different compositions, though suggestive, are not conclusive. In this regard, saturation concentrations of Ru in $MgTiO_3$ were found to be at the 3.5 wt% concentration level as well, which, in the absence of other considerations, might lead one to conclude that this provides an estimate of the amount of Ru^{4+} in the hematite system. It thus seems likely that the multivalency of both Fe and Ru play a significant role in the chemistry of this solid solution with the predominance of Fe^{3+} and Ru^{4+}.

Phase analysis and thermodynamics

Table 1 reports weight percent solubilities of Ru in hematite. These data represent the maximum concentrations of Ru that can be dissolved in hematite at 1 atm (Fig. 5). The data define a phase boundary for the terminal solid solution of Ru in hematite. This boundary is also constrained by the presence of two other solid phases, RuO_2 and Ru. Because the system has three components with three phases at constant pressure, the boundary is expected to be univariant. Although the RuO_2 and Ru phases must contain some Fe, microprobe analysis showed that Fe contents were always low, <1.5 wt% and typically <1 wt%.

A value for oxygen fugacity could in principle be calculated from the Fe concentrations in Ru and RuO_2 given accurate values for the appropriate Henry's Law constants of Fe in both Ru metal and RuO_2 oxide and their variations with temperature. A much simpler and more reliable method to calculate the relevant oxygen fugacity is to use the ratio of activities of the RuO_2 and Ru components in their respective phases, which in both phases are near one. The oxygen fugacity is then available through the expression for the equilibrium constant written for the reaction in Equation 3.

$$\frac{a_{RuO_2}^{oxide}}{a_{Ru}^{metal}} \exp(-\Delta G_{T,3}^{0}/RT) = f_{O_2} \quad (5)$$

Due to Raoult's Law, the activity ratio in Equation 5 is close enough to one to justify the simplification of buffering phases that were pure. For further simplification of subsequent analysis, heat capacity differences between reactants and products are ignored; in Equation 3 this makes very little difference to calculated oxygen fugacity over the experimental temperature range (a maximum of 0.07 log unit deviation from the mean value). Literature values (Kubaschewski and Alcock 1979) for the 298 K

enthalpy of formation of RuO_2 (−304600 J/mol) and for the 298 K entropies of phases in Equation 3 were used to estimate an entropy for that reaction [(172.9 J/(mol·K)], which were then combined to find $\Delta G^0_{T,3}$ in Equation 5. With these simplifications, Equation 5 can be substituted into an expression for the equilibrium constant of Equation 4, where the free energy is separated into enthalpy and entropy terms, to give:

$$\frac{-\Delta H^0_4 + \tfrac{1}{2}\Delta H^0_3}{RT} + \frac{\Delta S^0_4 - \tfrac{1}{2}\Delta S^0_3}{R} = \ln\frac{(a^{\text{oxide}}_{FeRuO_3})^2}{a^{\text{oxide}}_{Fe_2O_3}} \quad (6)$$

This equation describes the buffered redox reaction applicable to the solubility measurements reported here.

To better constrain the thermodynamic parameters to be fitted, ΔS^0_4 was approximated using known 298 K entropies for the participating phases and an estimate for the entropy of the hypothetical end-member phase, $FeRuO_3$. This hypothetical end-member is assumed to be disordered and of the hematite structure. In support of this, powder X-ray diffraction of run products always showed peaks for hematite solid solutions (plus Ru and RuO_2) and none to indicate a long-range ordered ilmenite-type phase. If an ordered, ilmenite-type compound exists in this system, then the critical temperature for ordering must be low enough that its formation is kinetically hindered. Thus, to estimate the entropy of the hypothetical hematite phase of $FeRuO_3$ stoichiometry, the systematics of Latimer's method were employed [see Kubaschewski and Alcock (1979)] to arrive at a 298 K entropy of 106.3 J/(mol·K). With these constraints, the standard state enthalpy of the reaction of Equation 4, ΔH^0_4, is the only free parameter on the left-hand side of Equation 6.

Considering that the solution of Ru in hematite is limited in extent to less than 34 wt% and that the solubility data are polythermal and fixed to a univariant curve it seemed appropriate to use only the simplest solution model. Thus, a strictly regular binary solution model was adopted:

$$\Delta H^{\text{mix}} = \alpha(1 - X_i)^2 + RT \ln X_i \quad (7)$$

In this model, the interaction parameter, α, is independent of temperature, permitting measured polythermal solubilities to be used to characterize α directly. Because the data is restricted to the Fe-rich side of the system and the solution model does not incorporate any other chemical or structural information, extrapolations outside the Fe-rich region of the solid solution are not meaningful. Fortunately, the Fe-rich region of this solid solution is of most interest to geochemistry and includes the Henry's Law region where $X_i \rightarrow 0$. In this model, Henry's Law constant is approximated by $\exp(\alpha/RT)$.

Substituting Equation 7 for component activities in Equation 6 and making use of the identity, $X_j = 1 - X_i$ for binary systems, one obtains:

$$\frac{-\Delta H^0_4 + \tfrac{1}{2}\Delta H^0_3}{RT} + \frac{\Delta S^0_4 - \tfrac{1}{2}\Delta S^0_3}{R} = \ln\frac{(X_{FeRuO_3})^2}{(1 - X_{FeRuO_3})} + \frac{\alpha}{RT}[2 - 4X_{FeRuO_3} + (X_{FeRuO_3})^2] \quad (8)$$

which can be used to determine ΔH^0_4 and α/R from experimental T and measured X_{FeRuO_3}. Fourteen pairs constrain the best-fit solid curve shown in Figure 5, which corresponds to: $\Delta H^0_4/R = 22620 \pm 90$ and $\alpha/R = 2230 \pm 60$. Error estimates are three standard deviations calculated from the trace of the variance-covariance matrix. These estimates are based only on the quality of the fit, i.e., the data points have not been weighted and the errors on the literature data used have not been incorporated.

Both fitted thermodynamic parameters converged on reasonable values. A significantly endothermic enthalpy for the reaction of Equation 4 is to be expected, considering the product side of the reaction contains both a gas and a phase that could not be synthesized and may not possess a stability field. The interaction parameter, α, is also endothermic, indicating positive deviations from ideal mixing. A subregular solution model, incorporating an excess entropy in addition to an excess enthalpy, was also fitted to the data and produced an excess enthalpy similar to the one-parameter fit and an excess entropy not statistically different from zero.

Brown and Navrotsky (1994) discussed some crystal-chemical controls on the enthalpies of mixing in the analogous system, Fe_2O_3-$FeTiO_3$. A sinusoidal enthalpy of mixing curve was found calorimetrically for a series of solid-solution samples across the entire binary join. They measured endothermic enthalpies for their hematite-rich solutions; this is analogous to the endothermic enthalpies inferred for the terminal solid solution investigated here. In the Ru-hematite system, however, the excess enthalpies, given by the regular solution formalism:

$$\Delta H^{\text{mix}} = \alpha(1 - X_{FeRuO_3})X_{FeRuO_3} \quad (9)$$

are considerably smaller than those measured calorimetrically in the Ti-rich hematites. For comparison, a subregular two-parameter fit to the calorimetric data of Brown and Navrotsky (1994) indicates approximately +8.8 kJ/mol excess enthalpy at 20 mol% ilmenite component, whereas Equation 9 predicts only +3.0 kJ/mol of excess enthalpy for the same amount of an Ru-bearing ilmenite component.

Ruthenium in hematite is apparently more stable than Ti in hematite. Perhaps this is in part due to the slightly smaller size mismatch between Fe^{3+} and Ru^{4+} compared Fe^{3+} and Ti^{4+}. If analogous chemical interactions exist between the two systems then some tendency toward an ilmenite-like ordered compound should exist. The small positive excess enthalpies indicated by the Ru solubility data may be due to a partial cancellation of a positive enthalpy of mixing by a smaller ordering enthalpy (Brown and Navrotsky 1994). In this case, short-range cation order, presumably a pairing of Fe^{2+} and Ru^{4+} across the shared octahedral face between cation layers, would reduce the energetically unfavorable mixing of Ru^{4+} within the cationic layers of Fe^{3+}. To assess this hypothesis, additional constraints on the mixing properties would be required, for instance, solution calorimetric data.

Ruthenium in oxides at lower oxygen fugacity

Solubility data reported in this study are limited by reduction to metallic Ru. The solubility curve shown in Figure 5 is therefore not a solvus, because there is no coexisting isostructural phase. The maximum measured solubility (34 wt% Ru), in terms of the Fe_2O_3-$FeRuO_3$ binary system, is 66 mol% $FeRuO_3$—two thirds the way toward a pure $FeRuO_3$ phase.

The enthalpy retrieved from Equation 4 (188.0 ± 0.7 kJ/mol) can be used to estimate an enthalpy of formation for the hypothetical disordered $FeRuO_3$ phase through the following relationship:

$$\Delta H^0_{\text{rnx 4}} = 2\Delta H^0_{\text{f, FeRuO}_3} + \tfrac{1}{2}\Delta H^0_{\text{f, O}_2} - 2\Delta H^0_{\text{f, RuO}_2} - \Delta H^0_{\text{f, Fe}_2\text{O}_3} \quad (10)$$

Taking enthalpies of formation of RuO_2 and Fe_2O_3 and combining them with the enthalpy of Equation 4, one calculates an enthalpy of formation from the elements for $FeRuO_3$ of −621.2 ± 0.8 kJ/mol, where only the experimental errors from this study have been propagated.

The estimate for the enthalpy of formation for the disordered Ru-bearing ilmenite phase allows calculations of Ru solubilities for other conditions. Although the chemical reaction of Equation 4 is useless for oxygen fugacity conditions below the stability of the RuO_2 phase, the following alternative reaction can be used to make estimates for minimum solubilities at geologically reasonable values of f_{o_2}:

$$2\text{Ru} + \tfrac{3}{2}\text{O}_2 + \text{Fe}_2\text{O}_3 = 2\text{FeRuO}_3 \quad (11)$$

Equation 11 cannot predict an accurate value for Ru concentrations at QMF in rhombohedral oxides because at QMF the ferric oxide component will be very small. To make an accurate estimate one would need to include reactions like Equation 11, but with Ru and an $FeTiO_3$ component.

Nevertheless, recognizing that a quantitative calculation of Ru solubility in Fe-Ti oxides must await further characterization of Ru solubilities in the Ti-bearing phase does not prohibit a qualitative assessment using the data obtained in this study. To this end, calculated estimates of Ru solubilities in a hypothetical rhombohedral oxide vs. temperature are plotted in Figure 6. These values are based on the following conditions: (1) saturation in Ru metal ($a_{Ru} = 1$); (2) oxygen fugacities given at each temperature by QMF or 3 log units above and below QMF; (3) an equilibrium constant for Equation 11, where ΔG^0_{11} includes estimates for $\Delta H^0_{\text{f, FeRuO3}}$ and S^0_{FeRuO3} obtained as explained above; (4) activity coefficients based on Equation 7 and the regular solution interaction parameter determined above; and (5) the effect of other components on the activity of $FeRuO_3$ being negligible. Figure 6 illustrates that oxidized Ru solubilities in the natural concentration range are plausible and that oxide phases may be sufficiently hospitable hosts to harbor appreciable amounts of PGE at magmatic conditions. Of course, this applies only in the absence of sulfides, or more rarely alloys, at which point the oxidic igneous geochemistry of Ru comes to an end.

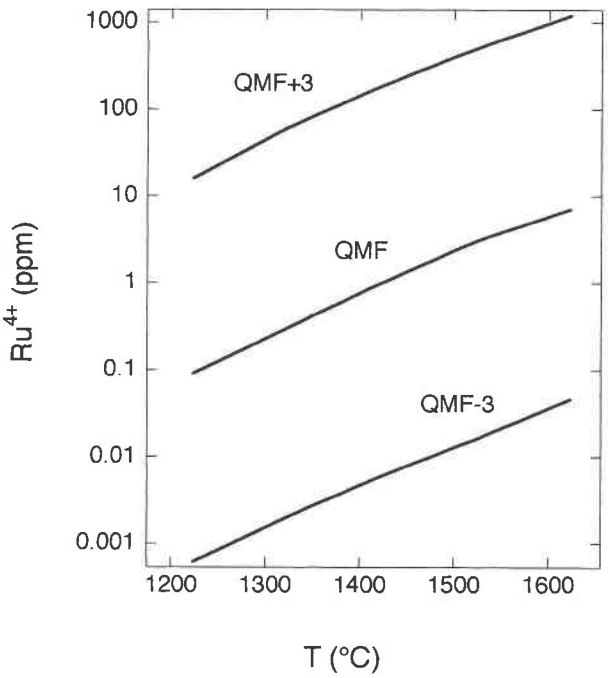

Figure 6. Calculated minimum solubilities of Ru^{4+} in a hypothetical rhombohedral oxide saturated by Ru metal at geologically reasonable values of f_{o_2} (QMF+3, QMF, and QMF-3) and temperatures (see text for caveats). Solubilities are based on a derived estimate for the enthalpy of formation of a hypothetical disordered $FeRuO_3$ phase and the non-ideal interaction of the $FeRuO_3$ component with Fe_2O_3. Note solubilities decrease with T and decreasing f_{o_2} but are well above typical primitive mantle concentrations (low parts per billion) for most conditions. At some low temperature, exsolution of metallic Ru is expected.

Finally, along redox buffering curves, as shown in Figure 6, solubilities decrease with decreasing temperature. At some low enough temperature, Ru metal should exsolve from the oxide. It may be that metallic Ru sometimes occurs due to exsolution from a previously dissolved condition as suggested long ago by Gijbels et al. (1974) for PGE alloys in chromite. This is not to suggest, however, that metallic Ru can only arise from exsolution within oxides. Metallic Ru may also appear from temperature dependent solubilities developing in sulfides (Peach and Mathez 1996) or other non-oxide phases with significant high temperature solubilities.

Conclusion

Ruthenium shows substantial substitutional solid solution into hematite at temperatures between 1000 and 1500 °C and at oxygen fugacities that are imposed by the coexistence of RuO_2 and Ru metal. Although experiments reported here do not demonstrate conclusively that Ru^{4+} is the dominant soluble species, there are several lines of evidence that lead to this conclusion. Nevertheless, a more rigorous thermodynamic characterization of this

system would be possible if the proportions of the possible species (Ru^{3+}, Ru^{4+}, Fe^{2+}, and Fe^{3+}) were better constrained, perhaps by Mössbauer spectroscopy, since oxidation states for both Ru and Fe can be analyzed by Mössbauer techniques.

An ordered ilmenite-type compound might have been expected in this system by analogy with the Fe_2O_3-$FeTiO_3$ system and the similarity of the ionic size mismatch between Fe^{2+}—Ti^{4+} (21%) and Fe^{2+}—Ru^{4+} (19%). None was found. This may simply mean that the critical temperature for ordering is below the experimentally investigated temperatures. In this case short-range cation order of ilmenite-type would be expected, at least in solid solutions formed at low temperature. On the other hand, the analogy to the Ti-bearing system may be inappropriate if, e.g., significant amounts Ru^{3+} participate in the solid solution. The ionic size difference between Ru^{3+} and Fe^{3+} (4%) is not large and would not lead to a large driving force for segregation into distinct cation layers, as in ilmenite. One speculative possibility is that the solid solution contains all four possible cations and that long-range ilmenite ordering is prevented by short-range order. Resolution of these possibilities must await further characterization of the cationic speciation within these solid solutions.

Finally, experiments reported here show that solid solubility of Ru in hematite does not produce large deviations from ideal behavior. Thus, the stability of an RuO_2 component, even at mantle conditions, may easily be great enough to permit a significant oxidic stage in the geochemistry of Ru in igneous systems.

Acknowledgments

This work was supported by NSF grants EAR-9706024 and EAR-9303676. Early discussions with Alex Navrotsky, Jiba Ganguly, and Kevin Righter are appreciated. I thank Ed Mathez and Mike Fleet for their helpful reviews.

References cited

Battle, P.D., Gibb, T.C., Jones, C.W., and Studer, F. (1989) Spin-glass behavior in Sr_2FeRuO_6 and $BaLaNiRuO_6$: A comparison with antiferromagnetic $BaLaZnRuO_6$. Journal of Solid State Chemistry, 78, 281–293.

Beer, H.B. (1980) The invention and industrial development of metal anodes. Journal of the Electrochemical Society, 127, 303C–307C.

Blazey, K.W., Müller, K.A., and Berlinger, W. (1985) Paramagnetic Ru^{5+} and Ru^{3+} centers in TiO_2: Ru. Solid State Communications, 54, 1039–1041.

Brown, N.E. and Navrotsky, A. (1994) Hematite-ilmenite (Fe_2O_3-$FeTiO_3$) solid solutions: The effects of cation ordering on the thermodynamics of mixing. American Mineralogist, 79, 485–496.

Capobianco, C.J. and Drake, M.J. (1990) Partitioning of ruthenium, rhodium and palladium between spinel and silicate melt. Geochimica et Cosmochimica Acta, 54, 869–874.

Capobianco, C.J., Hervig, R.L., and Drake, M.J. (1994) Experiments on crystal/liquid partitioning of Ru, Rh and Pd for magnetite and hematite solid solutions crystallized from silicate melt. Chemical Geology, 113, 23–43.

Dixon, S., Marr, J., Lachowski, E.E., Gard, J.A., and Glasser, F.P. (1980) Preparation and properties of some phases. Materials Research Bulletin, 15, 1811–1816.

Donohue, P.C., Katz, L., and Ward, R. (1966) The modification of structures of ternary oxides by cation substitution. I. Substitution of strontium for barium in barium ruthenium oxide and in barium iridium oxide. Inorganic Chemistry, 5, 335–338.

Gijbels, R.H., Millard Jr., H.T., Desborough, G.A., and Bartel, A.J. (1974) Osmium, ruthenium, iridium and uranium in silicates and chromite from the eastern Bushveld complex, South Africa. Geochimica et Cosmochimica Acta, 38, 319–337.

Greatrex, R., Greenwood, N.N., Lal, M., and Fernandez, I. (1979) A study of the ruthenium (V) perovskites M_2LnRuO_6 (M=Ca, Ln=Y, La, or Eu; M=Sr, Ln=Y; M=Ba, Ln=La or Eu) by ^{99}Ru Mössbauer spectroscopy and other techniques. Journal of Solid State Chemistry, 30, 137–148.

Hrovat, M., Holc, J., and Kolar, D. (1993) Phase equilibria in RuO_2—TiO_2—Al_2O_3 and RuO_2—TiO_2—Bi_2O_3 systems. Journal of Materials Science Letters, 12, 1858–1860.

Hrovat, M., Holc, J., Samardzija, Z., and Drazic, G. (1996) The extent of solid solubility in the RuO_2—TiO_2 system. Journal of Materials Research, 11, 727–732.

Hutson, N.D. (1994) The behavior of the platinum group metals in a borosilicate waste glass and their effects on the operation of a joule heated ceramic melter. In George B. Mellinger, Ed., Environmental and Waste Management Issues in the Ceramic Industry, p. 257–264. Ceramic Transactions, The American Ceramic Society, Westerville, Ohio.

Jantzen, C.M., Glasser, F.P., and Lachowski, E.E. (1981) Solid-state reactions of sintered commercial radwaste ceramics: I. Purex and Magnox wastes without additives. Materials Research Bulletin, 17, 77–87.

Kafalas, J.A. and Longo, J.M. (1970) Pressure-induced pyrochlore to perovskite transformations in the $Sr_{1-x}Pb_xRuO_3$ system. Materials Research Bulletin, 5, 193–198.

Kobayashi, H., Nagata, M., Kanno, R., and Kawamoto, Y. (1994) Structural characterization of the orthorhombic perovskites: [$ARuO_3$ (A=Ca, Sr, La, Pr)]. Materials Research Bulletin, 29, 1271–1280.

Kubaschewski, O. and Alcock, C.B. (1979) Metallurgical Thermochemistry. Pergamon Press, New York.

Lindsley, D.H. (1991) Experimental studies of oxide minerals. In Mineralogical Society of America Reviews in Mineralogy, 25, 69–106.

Longo, J.M. and Kafalas, J.A. (1968) Pressure-induced structural changes in the system $Ba_{1-x}Sr_xRuO_3$. Materials Research Bulletin, 3, 687–692.

O'Neill, H.St.C., Dingwell, D.B., Borisov, A., and Spettel, B.P. (1995) Experimental petrochemistry of some highly siderophile elements at high temperatures, and some implications for core formation and the mantle's early history. Chemical Geology, 120, 255–273.

Quilty, J., Trodahl, H.J., and Edgar, A. (1993) Raman spectroscopy of $BaRuO_3$. Solid State Communications, 86, 369–371.

Randall, J.J. and Ward, R. (1959) The preparation of some ternary oxides of the platinum metals. Journal of American Chemical Society, 81, 2629–2631.

Rard, J.A. (1985) Chemistry and thermodynamics of ruthenium and some of its inorganic compounds and aqueous species. Chemical Reviews, 85, 2–39.

Schreiber, H.D., Settle, F.A., Jamison, P.L., Eckenrode, J.P., and Headley, G.W. (1986) Ruthenium in glass-forming borosilicate melts. Journal of the Less-Common Metals, 115, 145–154.

Silverman, M.D. and Levy, H.A. (1954) Crystal structure of potassium perruthenate, $KRuO_4$. Journal of the American Chemical Society, 76, 3317–3319.

Triggs, P., Lévy, F., and Wagner, F.E. (1984) Mossbauer evidence for Ru(IV) and Ru(II) in TiO_2. Materials Research Bulletin, 19, 197–200.

van Berkel, F.P.F., Zandbergen, H.W., and IJdo, D.J.W. (1987) The system BaO-RuO_2-Al_2O_3 with less than 50 mol% BaO at 1300 °C. Materials Research Bulletin, 22, 165–168.

Westland, A.D. (1989) Inorganic chemistry of the platinum-group elements. In L.J. Cabri, Ed., Platinum-group elements: mineralogy, geology, recovery, p. 5–18. The Canadian Institute of Mining and Metallurgy, Montreal, Quebec.

Wiley, J.B. and Poeppelmeier, K.R. (1991) Reduction chemistry of platinum group metal perovskites. Materials Research Bulletin, 26, 1201–1210.

Williams, T., Lichtenberg, F., Reller, A., and Bednorz, G. (1991) New layered perovskites in the Sr-Ru-O system: A transmission electron microscope study. Materials Research Bulletin, 26, 763–770.

Manuscript received August 4, 1997
Manuscript accepted July 20, 1998
Paper handled by Craig Manning